View Online / Journal Homepage / Table of Contents for this issue

Organic & Biomolecular Chemistry

This article is part of the

OBC 10th anniversary

themed issue

All articles in this issue will be gathered together online at

www.rsc.org/OBC10

Downloaded by University of California - San Diego on 01 September 2012
Published on 16 February 2012 on http://pubs.rsc.org | doi:10.1039/C2OB00034B

Organic & Biomolecular Chemistry

Dynamic Article Links
View Online

Cite this: *Org. Biomol. Chem.*, 2012, **10**, 5764

www.rsc.org/obc

COMMUNICATION

Tuning and predicting biological affinity: aryl nitriles as cysteine protease inhibitors†‡§

Veronika Ehmke,[a] Jose Enrico Q. Quinsaat,[a] Pablo Rivera-Fuentes,[a] Cornelia Heindl,[b] Céline Freymond,[c,d] Matthias Rottmann,[c,d] Reto Brun,[c,d] Tanja Schirmeister[b,e] and François Diederich*[a]

Received 5th January 2012, Accepted 23rd January 2012
DOI: 10.1039/c2ob00034b

Published on 16 February 2012 on http://pubs.rsc.org | doi:10.1039/C2OB00034B
Downloaded by University of California - San Diego on 01 September 2012

A series of aryl nitrile-based ligands were prepared to investigate the effect of their electrophilicity on the affinity against the cysteine proteases rhodesain and human cathepsin L. Density functional theory calculations provided relative reactivities of the nitriles, enabling prediction of their biological affinity and cytotoxicity and a clear structure–activity relationship.

Four major classes of proteases selectively catalyse the hydrolysis of polypeptide bonds. Their general control over protein synthesis, turnover and function enables them to regulate many essential physiological processes.[1] Cysteine proteases utilise a catalytic thiolate that mediates protein hydrolysis by nucleophilic attack on the carbonyl group of the susceptible peptide bond. Among cysteine proteases, the enzymes of the papain-family use a catalytic dyad of cysteine and histidine for their proteolytic activity. They are among the best-characterised eukaryotic proteases and are involved in disease propagation and proliferation. Therefore, inhibitors are continuously emerging as promising therapeutic agents for example for the treatment of parasitic infections, as well as for inflammatory, immunological, cardiovascular and neurodegenerative disorders.[2]

Cysteine protease inhibitors have been traditionally developed by screening methods and subsequent lead optimisation.[2] They share as a common feature an electrophilic peptide bond isostere to react with the catalytic cysteine under formation of a covalent adduct.

Different functional groups that irreversibly alkylate or acylate the active site have been incorporated into a variety of ligands.[3] They often show, however, off-target effects and in particular cross-reactivity towards serine and other cysteine proteases. This has much hampered the therapeutic development of cysteine protease inhibitors despite the validation of these enzymes as drug targets. Only a limited number of electrophilic isosteres have found application as selective and reversibly-binding ligands.[3] The best-studied classes of reversible covalent inhibitors comprise aldehydes, certain ketones and few nitriles. Aldehydes and ketones, however, are more susceptible to side reactions because of their pronounced electrophilicity, whereas nitriles are generally less reactive. They form a covalent thioimidate adduct with the active site cysteine, which resembles the transition state of the amide bond hydrolysis.[4] Several nitrile-bearing cysteine protease inhibitors are in development and clinical trials, highlighting the relevance of the nitrile group as a pharmacophore in modern medicinal chemistry.[5]

Cysteine proteases of protozoan parasites have emerged as promising targets in drug development due to their indispensable role in the life cycle of the parasite.[6] According to the World Health Organisation (WHO), 3.5 billion people suffer from parasitic diseases, distributed predominantly in tropical areas of the world.[7] *Trypanosoma* (*T.*) *brucei* parasites cause human African trypanosomiasis (HAT, African sleeping sickness) leading to 50 000–70 000 infections annually. Over 60 million people live at risk of contracting the disease. Only four drugs are currently approved for treatment, however, widespread parasite resistance and severe toxicity issues drastically limit their application.[7] Bloodstream *T. brucei rhodesiense* parasites, causing the most acute form of the disease, express two papain-family cysteine proteases, which are directly implicated in the progression of the disease.[8] One of these enzymes is the highly abundant cathepsin L-like hydrolase rhodesain, which has been identified in all phases of the life-cycle, particularly during the infective stage of parasite development.[9] Cysteine protease inhibitors have been shown to cure infections in animal models, validating rhodesain as an interesting new target against HAT.[9,10]

Recently, we developed a series of potent peptidomimetic and triazine nitrile inhibitors against the parasitic cysteine proteases

[a]*Laboratorium für Organische Chemie, ETH Zürich, Hönggerberg, HCI, Wolfgang-Pauli-Strasse 10, 8093 Zurich, Switzerland. E-mail: diederich@org.chem.ethz.ch; Fax: (+41)44-632-1109*
[b]*Institute of Pharmacy and Food Chemistry, University of Würzburg, Am Hubland, 97074 Würzburg, Germany*
[c]*Swiss Tropical and Public Health Institute, Socinstrasse 57, 4002 Basel, Switzerland*
[d]*University of Basel, Petersplatz 1, 4003 Basel, Switzerland*
[e]*Institute of Pharmacy and Biochemistry, Johannes Gutenberg-University Mainz, Staudinger Weg 5, 55128 Mainz, Germany*

† Dedicated to Professor Wilfred van Gunsteren on the occasion of his 65th birthday.

‡ This article is part of the Organic & Biomolecular Chemistry 10th Anniversary issue.

§ Electronic supplementary information (ESI) available: Detailed experimental procedures and spectroscopic data for all compounds, biological assays and additional figures and tables. See DOI: 10.1039/c2ob00034b

This journal is © The Royal Society of Chemistry 2012

Downloaded by University of California - San Diego on 01 September 2012
Published on 16 February 2012 on http://pubs.rsc.org | doi:10.1039/C2OB00034B

falcipain-2 of *Plasmodium falciparum* and rhodesain by molecular modeling.[11] Starting from two available X-ray crystal structures of rhodesain,[9,12] molecular modeling using MOLOC[13] led to a diamino-substituted triazine as the central scaffold (Fig. 1).

Lead structure **1** showed an inhibitory constant (K_i) against rhodesain in the single-digit nanomolar range. The mainly hydrophobic S2 pocket was addressed with a cyclohexyl substituent, and a 1,3-benzodioxol-5-yl group was chosen to stack on the flat peptide backbone formed by Gly65 and Gly66, thereby filling the solvent exposed S3 pocket. Some compounds of the triazine library, however, showed low selectivity against the structurally closely related human cathepsin L (hCatL, **1**: K_i(hCatL) = 33 nM). More importantly, *in vitro* assays revealed cytotoxicity of the active ligands in the low micromolar range.[11a] We assumed that the strong electron-withdrawing effect of the triazine core enhanced the electrophilicity of the nitrile head group, making it more susceptible to off-target effects. Oballa *et al.* proposed a simple computational method to assess the relative electrophilicity of nitriles, which influences the reversibility of the adduct formation of nitriles with free cysteine.[14,15] In this work, we sought to establish a generally applicable, predictive structure–activity relationship (SAR) between experimentally determined enzyme inhibition and cytotoxicity data with calculated nitrile electrophilicities.

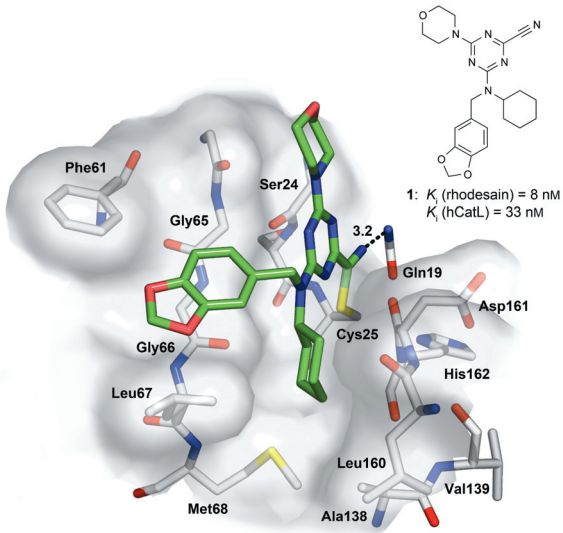

Fig. 1 Structure and binding mode of inhibitor **1** in the active site of rhodesain (PDB code: 2P86, resolution 1.16 Å) as generated with MOLOC. Colour code: C_{enzyme} grey, C_{ligand} green, O red, N blue, S yellow. Distance is given in Å.

Starting from lead compound **1**, first the effect of various heteroaromatic nitriles on rhodesain and hCatL inhibition was explored. A series of ligands **2–12** (Fig. 2) was prepared by varying the electronic properties of the central aromatic core, which in turn determine the electrophilicity of the nitrile head group. The S2 and S3 vectors were kept constant. Triazines **2** and **3** were prepared to evaluate the influence of the morpholine group of **1** on activation of the nitrile and inhibition. The number of electron-withdrawing N-atoms was subsequently reduced to two in ligands **4–9**, featuring pyrimidine, quinazoline and pyrazine cores, and to one in pyridine derivative **10**. Ligands with 5-membered heteroaromatic rings, such as thiazole **11** and oxazole **12**, completed the series. All ligands were designed to maintain a similar binding geometry at the enzyme active site to ensure that differences in biological affinity are mainly due to variation of the electronic properties of the aryl nitriles and not to other contacts with the enzyme (Fig. S1, ESI§).

For the synthesis of the ligands, triazine nitriles **2** and **3** were prepared according to the protocol reported for **1** (for details see ESI§).[11] Pyrimidine and quinazoline derivatives **4–8** were obtained following the sequence shown exemplarily for pyrimidines **5** and **7** in Scheme 1a. Nucleophilic aromatic substitution of amine **13** and 5-bromo-2,4-dichloropyrimidine gave pyrimidine **14**, which was converted into nitrile **5** using potassium cyanide and 1,4-diazabicyclo[2.2.2]octane (DABCO) in excellent yield. Methyl fluorosulfonyldifluoroacetate and copper(I) iodide were used to *in situ* generate trifluoromethylcopper[16] as the nucleophilic trifluoromethylating agent giving **7** in good yield. The syntheses of pyrazine **9** and pyridine **10** relied on Buchwald–Hartwig amination protocols[17] followed by

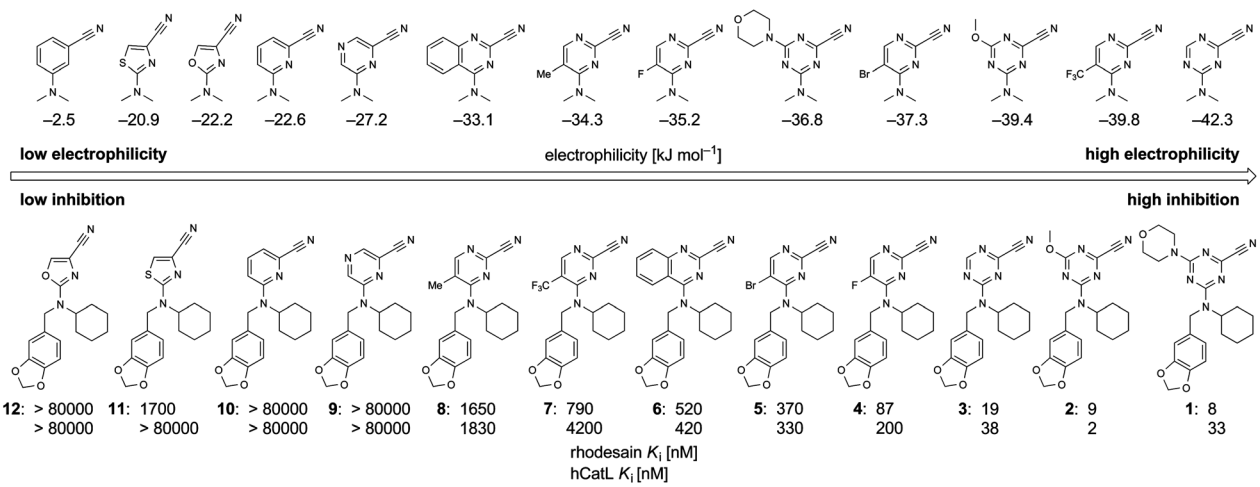

Fig. 2 Nitrile scale of calculated electrophilicities (level of theory: B3LYP/6-311G(d,p)) in kJ mol^{-1} of simplified aryl nitriles (top). Inhibition constants K_i of the corresponding ligands **1–12** are given in nanomolar against rhodesain and hCatL (bottom).

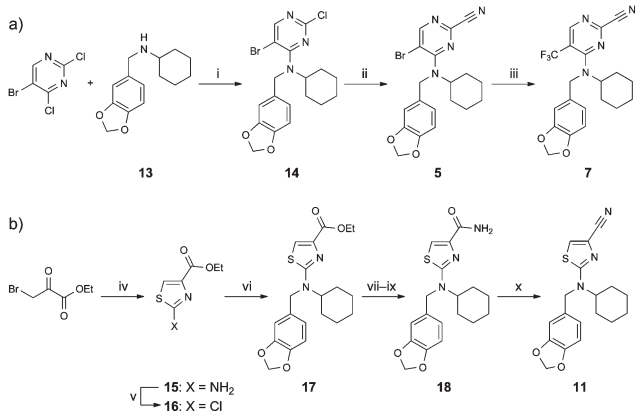

Scheme 1 (a) Synthesis of inhibitors **5** and **7**: (i) $^{i}Pr_2NEt$, $^{i}PrOH$, 80 °C, 18 h, 84%; (ii) KCN, DABCO, Me_2SO–H_2O 9 : 1, 120 °C, 2 h, 89%; (iii) methyl fluorosulfonyldifluoroacetate, CuI, HMPA, 80 °C, 2.5 h, 73%; (b) synthesis of inhibitor **11**: (iv) thiourea, EtOH, 85 °C, 1.5 h, 98%; (v) $CuCl_2$, $^{t}BuONO$, MeCN, 65 °C, 5.5 h, 27%; (vi) **13**, 1,4-dioxane, 120 °C, 7 d, 9%; (vii) LiOH·H_2O, THF–MeOH–H_2O 2 : 2 : 1, 40 °C, 3 h; (viii) $SOCl_2$, DMF, toluene, 80 °C, 1.5 h; (ix) NH_3–MeOH, toluene, 0→25 °C, 1 h, 66% (over 3 steps); (x) Burgess reagent (methyl *N*-(triethylammonium-sulfonyl)carbamate), CH_2Cl_2, 25 °C, 2 h, 82%; DABCO = 1,4-diaza-bicyclo[2.2.2]octane, HMPA = hexamethylphosphoramide.

palladium-catalysed cyanation with zinc(II) cyanide (see ESI§).[18] The 5-membered heteroaromatic nitriles **11** and **12** were obtained as outlined for thiazole **11** in Scheme 1b. A condensation reaction of thiourea and ethyl bromopyruvate gave quantitatively aminothiazole **15**, which was converted into 2-chlorothiazole **16** by a Sandmeyer reaction. Subsequent nucleophilic aromatic substitution by amine **13** gave ester **17** in poor yield due to the low electrophilicity of the 2-chlorothiazole ring. The ethyl ester was transformed into the corresponding amide **18**, and dehydration using Burgess reagent[19] gave nitrile **11** in high yield. Methyl fluorosulfonyldifluoroacetate and copper(I) iodide were used to *in situ* generate trifluoromethylcopper[16] as the nucleophilic trifluoromethylating agent giving **7** in good yield. The syntheses of pyrazine **9** and pyridine **10** relied on Buchwald–Hartwig amination protocols[17] followed by palladium-catalysed cyanation with zinc(II) cyanide (see ESI§).[18] The 5-membered heteroaromatic nitriles **11** and **12** were obtained as outlined for thiazole **11** in Scheme 1b. A condensation reaction of thiourea and ethyl bromopyruvate gave quantitatively aminothiazole **15**, which was converted into 2-chlorothiazole **16** by a Sandmeyer reaction. Subsequent nucleophilic aromatic substitution by amine **13** gave ester **17** in poor yield due to the low electrophilicity of the 2-chlorothiazole ring. The ethyl ester was transformed into the corresponding amide **18**, and dehydration using Burgess reagent[19] gave nitrile **11** in high yield.

We used density functional theory (DFT) calculations to assess the relative reactivities of the nitrile groups attached to different heteroaryl scaffolds towards a sulfur nucleophile, in order to predict the biological affinities of the new nitrile-based inhibitors against rhodesain and hCatL. The electrophilicities were calculated as the formation enthalpies of the thioimidate adducts formed in a theoretical reaction between methanethiol and aryl nitriles similarly to the method reported by Oballa *et al.*

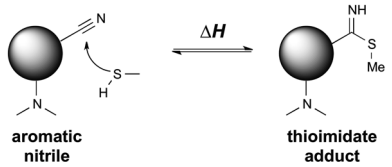

Scheme 2 Model reaction of a simplified aromatic nitrile with methanethiol resulting in a thioimidate adduct. Relative electrophilicities are calculated as $\Delta H_{thioimidate} - (\Delta H_{nitrile} + \Delta H_{methanethiol})$. ΔH values were obtained at the B3LYP/6-311G(d,p) level of theory.

(Scheme 2).[14] The aryl nitriles were structurally based on ligands **1–12**, but simplified concerning the S2 and S3 substituents (Fig. 2, top). The structures of methanethiol, the simplified nitriles and the corresponding thioimidate adducts were optimised in water (PCM solvation model) at the B3LYP/6-311G (d,p) level of theory using Gaussian 09.[20] The resulting electrophilicity index corresponds to the differences in formation enthalpies $\Delta H_{thioimidate} - (\Delta H_{nitrile} + \Delta H_{methanethiol})$ and is given in kJ mol^{-1}. The values obtained give only thermodynamic information within the model reaction and therefore should only be used to qualitatively arrange and rank the aryl nitriles.

The scale of electrophilicity values of the designed aromatic nitriles as obtained by DFT calculations is shown in Fig. 2 (top). Very negative values indicate high electrophilicity in accordance with the equilibrium of the model reaction, whereas small negative values are attributed to poor electrophilicity. As expected, triazine nitriles are predicted to be highly reactive towards nucleophiles due to their pronounced electron-withdrawing effect (−42.3 to −36.8 kJ mol^{-1}). Electrophilicities of pyrimidine and quinazoline-based nitriles span a wide range from strongly activated in the trifluoromethylated analogue (−39.8 kJ mol^{-1}) to intermediate activation for the quinazoline compound (−33.1 kJ mol^{-1}). Pyrazine and pyridine nitriles are only moderately reactive towards nucleophiles (−27.2 and −22.6 kJ mol^{-1}). Finally, 5-membered heteroaromatic systems are in a similar intermediate range due to their electron-rich aromatic system. The unactivated benzonitrile analogue (−2.5 kJ mol^{-1}) and other heterocyclic aromatic nitriles covering the range from −16.5 to −1.2 kJ mol^{-1} (not shown in Fig. 2) were included to complete and verify the scale (for the extended electrophilicity scale see Table S1, ESI§). This approach provides a useful and straightforward measure of the relative electrophilicities and can be generally applied to aryl nitrile systems.

Nitriles **1–12** were subsequently tested against rhodesain from *T. brucei rhodesiense* and hCatL (see ESI§) in order to correlate the calculated electrophilicities to the biological affinities of the covalent reversible nitrile ligands. Inhibitory constants against rhodesain and hCatL span from single-digit nanomolar for triazine ligands **1** and **2** to >80 μM for nitriles **9–12**. In Fig. 2 (bottom), all ligands are arranged according to their inhibitory constants. Noticeably, this alignment is in accordance with the nature of the central core and leads to grouping of the corresponding heteroaromatic rings (triazines > pyrimidines/quinazolines > pyrazine/pyridine/thiazole/oxazole). Moreover, the biological results correlate very well with the calculated electrophilicities of our model system. Strongly activated nitriles present in triazines **1–3** lead to highly potent inhibition against

Published on 16 February 2012 on http://pubs.rsc.org | doi:10.1039/C2OB00034B
Downloaded by University of California - San Diego on 01 September 2012

 This journal is © The Royal Society of Chemistry 2012

Published on 16 February 2012 on http://pubs.rsc.org | doi:10.1039/C2OB00034B
Downloaded by University of California - San Diego on 01 September 2012

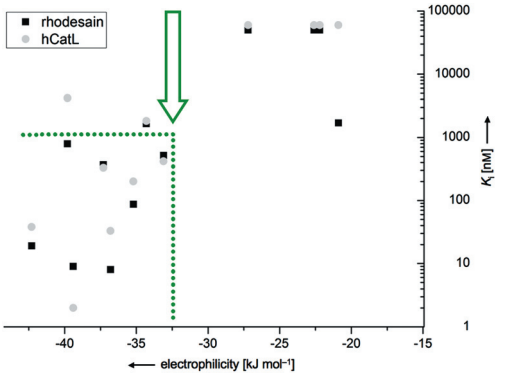

Fig. 3 Inhibition constants K_i in nanomolar of nitrile ligands **1–12** against rhodesain (black squares) and hCatL (grey spheres) plotted against the calculated electrophilicities in kJ mol^{-1}. The *y*-axis is shown as a logarithmic scale. The threshold at −33 kJ mol^{-1} (green) marks the limit for nanomolar inhibition.

both rhodesain (**1**: K_i(rhodesain) = 8 nM, **2**: K_i(rhodesain) = 9 nM, **3**: K_i(rhodesain) = 19 nM) and hCatL (**1**: K_i(hCatL) = 33 nM, **2**: K_i(hCatL) = 2 nM, **3**: K_i(hCatL) = 38 nM). For pyrimidine and quinazoline ligands **4–8**, moderate to high inhibition is predicted according to their electrophilicities. Indeed, nitriles **4–8** inhibited rhodesain and hCatL with K_i values ranging from 87 nM to low micromolar. Less activated nitriles, such as pyrazine **9**, pyridine **10**, thiazole **11** and oxazole **12**, showed no or only low inhibition, as predicted by the calculated low electrophilicities. This SAR validates the results obtained by the DFT calculations and confirms the initial hypothesis that biological affinity is strongly influenced by the electronic nature of the nitrile. In order to obtain potent ligands with nanomolar or very low micromolar inhibitory constants, a certain electrophilicity of the head group is required (Fig. 3). The threshold for both rhodesain and hCatL lies below an activation of the nitrile of around −33 kJ mol^{-1}. The data indicate that the calculated electrophilicity is useful in reliably predicting the order of magnitude of inhibitory constants against the investigated cysteine proteases. The only exemption in the ligand series comprised trifluoromethyl-substituted pyrimidine **7**, for which higher inhibition would have been expected. This might be due to unfavourable, allyl 1,3-strain-type intramolecular repulsions between the sterically demanding CF_3 substituent and the benzylic CH_2 group, leading to a loss in binding affinity (Fig. S2, ESI§).

Cell proliferation inhibition was assessed for compounds **1–12** using rat skeletal myoblast (L-6) cells in order to study the direct influence of the electrophilicity on cytotoxicity. The aryl nitrile ligands showed in general low cytotoxicity with IC_{50} values between 5.6 to 43.0 μM and revealed an excellent correlation to the calculated electrophilicities (Table 1). Aryl nitriles with high electrophilicity such as triazines **2** and **3** and pyrimidine **7** showed the lowest IC_{50} values against L-6 cells (**2**: IC_{50} = 5.6 μM, **3**: IC_{50} = 6.7 μM, **7**: IC_{50} = 6.0 μM). Thiazole **11** and oxazole **12**, featuring a much less reactive nitrile group, exhibited a 5-fold lower cytotoxicity with IC_{50} values of 31.5 and 43.0 μM, respectively. These data clearly indicate that reduced electrophilicity leads to reduced cytotoxicity, which is in agreement with the correlation found for the inhibition constants against rhodesain and hCatL. The electrophilicity scale can therefore also be applied to give an indication of the cytotoxicity of cysteine protease inhibitors, even though other aspects such as pharmacokinetic properties of the compounds need to be considered.

Table 1 Cytotoxicity of compounds **1–12** and calculated electrophilicities.[a] The compounds are arranged according to their theoretical electrophilicities

Electrophilicity [kJ mol^{-1}]	Compound	Cytotoxicity L-6[b] IC_{50} [μM]
−42.3	**3**	6.7
−39.8	**7**	6.0
−39.4	**2**	5.6
−37.3	**5**	10.3
−36.8	**1**	11.1
−35.2	**4**	20.0
−34.3	**8**	19.0
−33.1	**6**	23.0
−27.2	**9**	24.0
−22.6	**10**	22.6
−22.2	**12**	43.0
−20.9	**11**	31.5

[a] All values represent the mean of at least two independent measurements, each performed in duplicate. [b] Rat skeletal myoblasts were used to assess cytotoxicity. Podophyllotoxin served as positive control in the assay (IC_{50} = 0.0082 μM).

In conclusion, we studied the SAR of aryl nitriles as covalent reversible inhibitors of rhodesain and hCatL. A series of ligands were designed and synthesised with varying aromatic cores to investigate the influence of the electronic properties of the nitrile on inhibition and cytotoxicity. DFT calculations of the nitrile electrophilicities were used to predict the affinity of the ligands against cysteine proteases and also their cytotoxicity. The method proved to be powerful in its simplicity, allowing the direct comparison of electrophilicities of related nitrile-bearing compounds. This nitrile scan was validated by a clear correlation of the activation of the head group to the inhibitory constants and cytotoxicity. Furthermore, the electrophilicity scale enabled us to predict biological affinities according to the electronic nature of the nitrile and will guide and simplify future optimisations of cysteine protease inhibitors. The further development towards a safe drug for HAT treatment in our laboratory will take into account these findings and rely on a multidimensional approach, optimising molecular recognition properties of the ligands to gain additional affinity from binding to the S2 and S3 sub-pockets and reducing in parallel the electrophilicity of the nitrile head group.

Acknowledgements

V.E. is grateful for a Kekulé fellowship of the German Fonds der Chemischen Industrie and P.R.-F. for a doctoral fellowship of the *Stipendienfonds der Schweizerischen Chemischen Industrie* (SSCI). Financial support by the Deutsche Forschungsgemeinschaft (SFB 630, TP A4, for T.S.) and the Swiss National Science Foundation is gratefully acknowledged. We thank

View Online

Dr Daniel Bur (*Actelion Pharmaceuticals Ltd., Basel*) for helpful discussions.

References

1 (*a*) D. Leung, G. Abbenante and D. P. Fairlie, *J. Med. Chem.*, 2000, **43**, 305–341; (*b*) B. Turk, *Nat. Rev. Drug Discovery*, 2006, **5**, 785–799.
2 (*a*) F. Lecaille, J. Kaleta and D. Brömme, *Chem. Rev.*, 2002, **102**, 4459–4488; (*b*) H.-H. Otto and T. Schirmeister, *Chem. Rev.*, 1997, **97**, 133–171; (*c*) M. Drag and G. S. Salvesen, *Nat. Rev. Drug Discovery*, 2010, **9**, 690–701.
3 R. Vicik, M. Busemann, K. Baumann and T. Schirmeister, *Curr. Top. Med. Chem.*, 2006, **6**, 331–353.
4 E. Dufour, A. C. Storer and R. Ménard, *Biochemistry*, 1995, **34**, 9136–9143.
5 F. F. Fleming, L. Yao, P. C. Ravikumar, L. Funk and B. C. Shook, *J. Med. Chem.*, 2010, **53**, 7902–7917.
6 M. Klemba and D. E. Goldberg, *Annu. Rev. Biochem.*, 2002, **71**, 275–305.
7 R. Brun, J. Blum, F. Chappuis and C. Burri, *Lancet*, 2010, **375**, 148–159.
8 J. H. McKerrow, E. Sun, P. J. Rosenthal and J. Bouvier, *Annu. Rev. Microbiol.*, 1993, **47**, 821–853.
9 I. D. Kerr, P. Wu, R. Marion-Tsukamaki, Z. B. Mackey and L. S. Brinen, *PLoS Negl. Trop. Dis.*, 2010, **4**, e701.
10 C. R. Caffrey, S. Scory and D. Steverding, *Curr. Drug Targets*, 2000, **1**, 155–162.
11 (*a*) V. Ehmke, C. Heindl, M. Rottmann, C. Freymond, W. B. Schweizer, R. Brun, A. Stich, T. Schirmeister and F. Diederich, *ChemMedChem*, 2011, **6**, 273–278; (*b*) V. Ehmke, F. Kilchmann, C. Heindl, K. Cui, J. Huang, T. Schirmeister and F. Diederich, *Med. Chem. Commun.*, 2011, **2**, 800–804.
12 I. D. Kerr, J. H. Lee, C. J. Farady, R. Marion, M. Rickert, M. Sajid, K. C. Pandey, C. R. Caffrey, J. Legac, E. Hansell, J. H. McKerrow, C. S. Craik, P. J. Rosenthal and L. S. Brinen, *J. Biol. Chem.*, 2009, **284**, 25697–25703.
13 P. R. Gerber and K. Müller, *J. Comput.-Aided Mol. Des.*, 1995, **9**, 251–268.
14 R. M. Oballa, J.-F. Truchon, C. I. Bayly, N. Chauret, S. Day, S. Crane and C. Berthelette, *Bioorg. Med. Chem. Lett.*, 2007, **17**, 998–1002.
15 For recent examples on experimentally determined electrophilic reactivity scales, as opposed to the electrophilicity scale described herein, see: (*a*) R. Appel and H. Mayr, *J. Am. Chem. Soc.*, 2011, **133**, 8240–8251; (*b*) M. Horn and H. Mayr, *Eur. J. Org. Chem.*, 2011, 6470–6475.
16 M. A. McClinton and D. A. McClinton, *Tetrahedron*, 1992, **48**, 6555–6666.
17 J. M. Coterón, D. Catterick, J. Castro, M. J. Chaparro, B. Díaz, E. Fernández, S. Ferrer, F. J. Gamo, M. Gordo, J. Gut, L. de las Heras, J. Legac, M. Marco, J. Miguel, V. Muñoz, E. Porras, J. C. de la Rosa, J. R. Ruiz, E. Sandoval, P. Ventosa, P. J. Rosenthal and J. M. Fiandor, *J. Med. Chem.*, 2010, **53**, 6129–6152.
18 F. Jin and P. N. Confalone, *Tetrahedron Lett.*, 2000, **41**, 3271–3273.
19 S. Khapli, S. Dey and D. Mal, *J. Indian Inst. Sci.*, 2001, **81**, 461–476.
20 M. J. Frisch, *et al.*, *GAUSSIAN 09 (Revision A.02)*, Gaussian, Inc., Wallingford CT, 2009 (for the full reference, see ESI§).

Downloaded by University of California - San Diego on 01 September 2012
Published on 16 February 2012 on http://pubs.rsc.org | doi:10.1039/C2OB00034B

 This journal is © The Royal Society of Chemistry 2012